atmosphere

MDPI

Article

Characteristics and Formation Mechanisms of Fine Particulate Nitrate in Typical Urban Areas in China

Xinlei Ge [1,*], Yanan He [1], Yele Sun [2], Jianzhong Xu [3], Junfeng Wang [1], Yafei Shen [1] and Mindong Chen [1]

1 Jiangsu Key Laboratory of Atmospheric Environment Monitoring and Pollution Control (AEMPC), Collaborative Innovation Center of Atmospheric Environment and Equipment Technology (CIC-AEET), School of Environmental Science and Engineering, Nanjing University of Information Science & Technology, Nanjing 210044, China; 13057589806@163.com (Y.H.); Njwangjunfeng@gmail.com (J.W.); shen1225@nuist.edu.cn (Y.S.); chenmd@nuist.edu.cn (M.C.)

2 State Key Laboratory of Atmospheric Boundary Layer Physics and Atmospheric Chemistry, Institute of Atmospheric Physics, Chinese Academy of Sciences, Beijing 100029, China; sunyele@mail.iap.ac.cn

3 State Key Laboratory of Cryospheric Sciences, Northwest Institute of Eco-Environment and Resources, Chinese Academy of Sciences, Lanzhou 730000, China; jzxu@lzb.ac.cn

* Correspondence: caxinra@163.com; Tel.: +86-25-5873-1394

Academic Editor: Guey-Rong Sheu

Received: 17 January 2017; Accepted: 20 March 2017; Published: 22 March 2017

Abstract: Nitrate is a very important aerosol component, thus elucidation of its characteristics and formation mechanisms is essential and important for effective reduction of aerosol pollution. In this work, highly time-resolved submicron aerosol (PM_1) data measured by Aerodyne aerosol mass spectrometers (AMS) in Nanjing, Beijing and Lanzhou during both summer and winter were integrated to investigate the nitrate behaviors in urban China air. Results showed that nitrate occupied 1/8–1/4 of PM_1 mass, typically higher than those observed in rural/remote regions. Relative mass fractions of nitrate also varied significantly at different pollution levels. Nitrate mass fractions generally increased with the increase of PM_1 loadings during summer, while the contributions during winter increased first and then decreased with the increase of pollution levels. We further propose that there are at least three mechanisms that likely govern the urban nitrate behaviors: Type I—thermodynamics driven, Type II—photochemistry driven, and Type III—planetary boundary layer (PBL) dynamics driven. Analyses of the ammonium-sulfate-nitrate data revealed that ammonium nitrate was able to form before sulfuric acid was fully neutralized in some urban areas. Our findings provide useful insights into the characterization and reduction of fine particulate nitrate pollution.

Keywords: fine aerosols; nitrate; aerosol mass spectrometer; diurnal variation; formation mechanism

1. Introduction

Fine particulate matter ($PM_{2.5}$) pollution is a very serious and pressing environmental issue in the densely populated areas of China [1–3]. $PM_{2.5}$ also has profound effects on the visibility, air quality, human health, and the Earth's climate, etc. Nitrate is one of the major components of $PM_{2.5}$, which can account for 4.5%–25% of the $PM_{2.5}$ mass, depending upon locations and environments [4–7]. Previous studies also showed that nitrate contributions to $PM_{2.5}$ mass could increase with the increase of $PM_{2.5}$ mass loadings [8]. Indeed, nitrate was found to be an very important contributor to the high $PM_{2.5}$ concentrations during heavy haze events in China [9]. In this regard, elucidation of the atmospheric behaviors of nitrate is critical to reduce the $PM_{2.5}$ pollution.

Nitrate may associate with different cations in the particle phase. Under marine environments, it may be partially present as $NaNO_3$ due to the reaction: $HNO_3 + NaCl = NaNO_3 + HCl$, but this reaction mainly affects the coarse particles [10] rather than fine particles ($PM_{2.5}$). Typically, fine aerosol nitrate exists in the form of ammonium nitrate, which is generated by the neutralization reaction: $HNO_3 + NH_3 = NH_4NO_3$. The precursor nitric acid (HNO_3) is overwhelmingly produced by secondary oxidation processes, and only a very small portion is emitted directly, for example, from volcano eruptions [11]. The secondary formation of HNO_3 includes two major pathways. During daytime, HNO_3 is mainly produced from OH-initiated oxidation of NO_2 [12]. During nighttime, NO_2 can be oxidized by O_3 to form NO_3 radical, which then reacts with NO_2 to form N_2O_5 [13]; N_2O_5 then heterogeneously reacts with water vapor on the particle surface and produces HNO_3 (this process is favored by low temperature and high relative humidity) [14,15]. Even when HNO_3 is available, the neutralization of HNO_3 with NH_3 can only occur efficiently under ammonium-rich conditions, as NH_3 prefers to react with sulfuric acid (H_2SO_4) first [16]. Some earlier studies [17,18] demonstrate that a molar ratio of NH_4^+/SO_4^{2-} larger than 1.5 can be treated as an ammonium-rich condition, meaning that NH_4NO_3 can be produced effectively after the formation of $(NH_4)_3H(SO_4)_2$. Nevertheless, this boundary value (1.5) may change as both homogenous and heterogeneous formations of NH_4NO_3 are possible in the real atmosphere [19], and the dominant pathway may vary at different locations, or during different seasons in the same location [20].

Traditionally, atmospheric particles are collected onto filters, and then nitrate concentration is determined by using ion chromatography (IC). Such nitrate data has low time resolution, as the filters are collected every few hours or days. From the year 2000, Aerodyne aerosol mass spectrometers (AMS) [21,22], which can determine the aerosol compositions quickly and in real-time, were used widely around the world. Due to the relatively simple fragmentation pattern in the AMS ionization scheme, ammonium nitrate is recommended as a standard mass calibration material for all versions of AMS, and the AMS is able to quantify nitrate relatively well. Given that the AMS also provides highly-time resolved data, it is particularly useful for investigating the temporal variations and diurnal cycles of nitrate. In this study, we integrated and analyzed the AMS data collected from a few typical cities in China (Nanjing, Beijing, and Lanzhou) during both summer and winter. The purpose of this work is to provide an overview of the characteristics of ambient aerosol nitrate in typical urban areas of China, and propose the dominant mechanisms that govern such nitrate characteristics under different atmospheric environments. Our findings can help researchers interpret the nitrate behaviors in future studies, and provide useful insights into the effective reduction of particulate nitrate pollution.

2. Experiments

In this work, we selected Nanjing, Beijing, and Lanzhou—three cities representing Yangtze River Delta (YRD), Beijing-Tianjin-Hebei (Jing-Jin-Ji), and northwestern part of China, respectively—for our sampling locations. The sampling locations, sampling periods, and the versions of Aerodyne AMS used for these field campaigns are shown in Figure 1. For Nanjing, a soot-particle AMS (SP-AMS) [23,24] was deployed in urban Nanjing (Jiangxin Island) from 11 August to 18 September 2014, and in the campus of Nanjing University of Information Science and Technology (NUIST) from 20 February to 23 March 2015 (details in [25]). For Beijing, an Aerosol Chemical Speciation Monitor [26] (ACSM, a simplified version of Aerodyne AMS) was deployed during summer (26 June–28 August 2011) and winter (21 November 2011–20 January 2012), both at the Institute of Atmospheric Physics (IAP) of Chinese Academy of Sciences (CAS). For Lanzhou, the measurements were performed by using a high resolution time-of-flight AMS (HR-ToF-AMS) [27] in the Cold and Arid Regions Environmental and Engineering Research Institute (CAREERI) during summer (11 July–7 August 2012) and at Lanzhou University during winter (10 January–4 February 2014) (the two sites are only about 500 meters apart). Note that the results of the Beijing summer data have been published in Sun et al. [28], and winter data was presented in Sun et al. [29,30], while results of Lanzhou summer and winter were presented in Xu et al. [31] and Xu et al. [32], respectively. The nitrate data from Beijing and Lanzhou were re-visited

here, together with the new Nanjing data, to unravel the aerosol nitrate behaviors and governing factors in different representative urban areas of China.

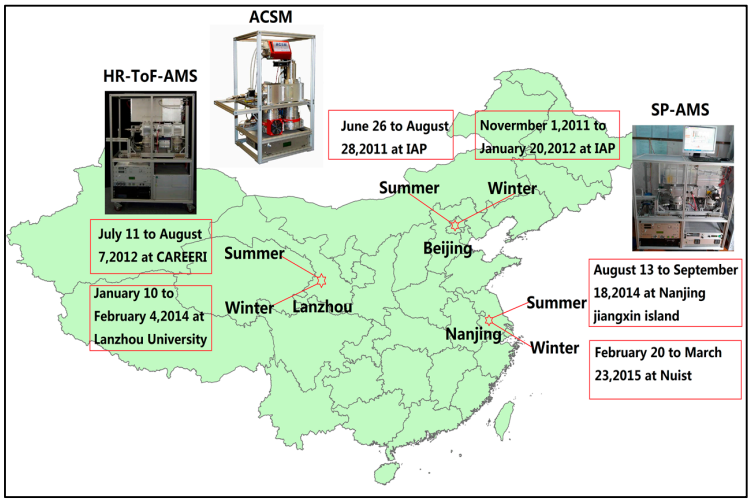

Figure 1. Sampling periods, locations, and aerosol mass spectrometers (AMS) versions of the datasets used in this work.

Due to the limitation of transmission efficiency of the AMS lens, AMS is able to measure particles mainly in the submicron meter range, and species that can vaporize at ~600 °C, thus the AMS-measured particles are referred to as non-refractory PM_1 (NR-PM_1) [21]. During the aforementioned field measurements, although different types of AMS were deployed, all of them (SP-AMS, ACSM, and HR-ToF-AMS) used ammonium nitrate to conduct the mass calibration, since it is easy to evaporate and has a very simple fragmentation pattern (mainly *m/z* 30—NO^+, and *m/z* 46—NO_2^+ from nitrate). The AMS is thus powerful in quantifying nitrate unless there are large amounts of organic or metal nitrates, since they can affect NO^+ and NO_2^+ signals significantly [33]. Quantification of other aerosol components, including sulfate, chloride, ammonium, and total organics, were all based on their relative ionization efficiencies to nitrate. Only SP-AMS can simultaneously determine the refractory black carbon (*r*BC) mass, since it is equipped with an additional laser vaporizer, and such *r*BC data were included here for Nanjing datasets. For Lanzhou, a multi-angle absorption photometer (MAAP) and a single-particle intracavity laser-induced incandescence photometer (SP2) were used to measure *r*BC during summer and winter, respectively [31,32]. No *r*BC mass concentrations were available for the Beijing datasets. The total organics can be further segregated into a few factors/sources (primary sources including traffic, cooking, biomass burning, coal combustion, etc., and secondary sources) via positive matrix factorization (PMF) [34,35]. Other supporting data included the meteorological parameters (temperature, relative humidity—RH, wind speed and direction, pressure, precipitation, and solar radiation) and concentrations of the gaseous pollutants (CO, SO_2, O_3, NO_2).

3. Results and Discussion

3.1. Average Mass Contributions, Diurnal Patterns, and Driving Factors

Figure 2 shows the campaign-averaged mass contributions of nitrate to the total PM_1 (left panel) and the corresponding diurnal cycles of nitrate concentrations (right panel) during summer and winter, in Nanjing, Beijing, and Lanzhou, respectively. It is clear that for these three cities, the PM_1 pollutions were all heavier during winter than during summer. This result is consistent with the air pollution status in most cities of China [3]. Nitrate concentrations were also elevated in winter—11.1 $\mu g/m^3$ (winter) versus 3.4 $\mu g/m^3$ (summer) in Nanjing and 7.2 $\mu g/m^3$ (winter) versus 3.9 $\mu g/m^3$ (summer) in Lanzhou, but in Beijing, nitrate mass loading was slightly higher during summer than it during winter

(12.4 versus 10.9 μg/m^3, respectively). The mass fractions of nitrate also increased during winter compared with those during summer in Nanjing and Lanzhou, while the fractions decreased during winter from those during summer in Beijing, mainly due to the increased contributions from organic constituents. Overall, we find that in urban areas of China, aerosol nitrate can occupy ~1/8 to ~1/4 of the total PM_1 mass based on the measurements shown here. This relative contribution of nitrate is generally within the range observed in other urban/suburban areas, but is typically higher than those measured in rural or remote areas [36]. This finding clearly shows that urban traffic emissions are the key factor to nitrate formation and thus represent an important contributor to the aerosol pollution in China.

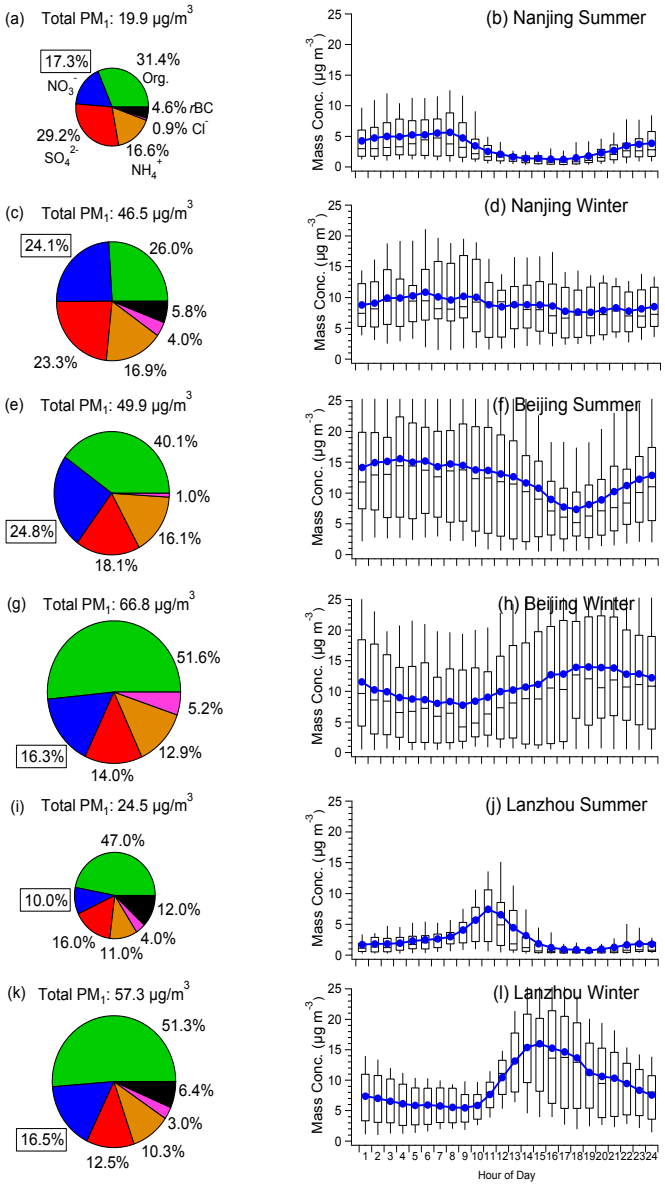

Figure 2. Average fine aerosol particulate matter (PM_1) mass loadings, chemical compositions and diurnal variations of the mass concentrations of nitrate: (**a**,**b**) Nanjing summer, (**c**,**d**) Nanjing winter, (**e**,**f**) Beijing summer, (**g**,**h**) Beijing winter, (**i**,**j**) Lanzhou summer, and (**k**,**l**) Lanzhou winter (Beijing datasets did not include refractory black carbon (*r*BC); the whiskers above and below the boxes are the 90th and 10th percentiles, the upper and lower boundaries of the boxes are the 75th and 25th percentiles, and the lines in the boxes indicate the median values and the dots indicate the mean values; note Figure 2e–l are reproduced and modified from previous studies [28,29,31,32]).

The AMS measurement has a very fine time resolution. For the field measurements included in this work, the sampling resolutions were 5 to 30 min, allowing us to derive the average diurnal cycles of nitrate which cannot be obtained from filter-based studies. As shown in Figure 2, the diurnal patterns of nitrate presented different behaviors among different cities and seasons. In Nanjing, nitrate varied relatively less during winter than it did during summer, overall, both seasons presented a similar trend—peaking in early morning and reaching minimum in the afternoon. In fact, this pattern was also observed by prior studies conducted during spring [24], autumn [37], and winter in urban Nanjing [38], suggesting that this behavior is similar throughout the year in Nanjing. For Beijing, summer nitrate concentrations responded similarly to the trends observed in the summer in Nanjing, while during winter, Beijing's nitrate concentrations displayed an opposite trend—peaking in the late afternoon/early evening (~7–8 p.m.) and dropping to minimum values in the early morning. This wintertime diurnal pattern was confirmed by another study conducted later in the same site [39]. Sun et al. [40] also conducted one-year continuous aerosol measurement, and found that the nitrate diurnal patterns differed greatly among different seasons, but that the afternoon increase only appeared during winter, indicating a specific wintertime nitrate formation pathway in Beijing. In case of Lanzhou, during summer, nitrate concentrations displayed a sharp peak in the morning (~10–11 a.m.), then gradually decreased to relatively low levels at other times; during winter, the diurnal cycle was somewhat similar to that observed in Beijing during winter, but changed more dramatically and peaked earlier (about 3 p.m.). This afternoon nitrate peak in Lanzhou was also observed by another AMS campaign conducted during 27 October to 3 December 2014 [41].

In order to elucidate the dominant factors that drive the different nitrate diurnal cycles presented above, we further calculated the diurnal variations of temperature, RH, solar radiation, and appended them along with that of nitrate for the six datasets in Figure 3. We also computed the theoretical dissociation constants of NH_4NO_3 (K_p) by assuming the system was at thermodynamic equilibrium. For Nanjing summer, nitrate varied closely with K_p (r = 0.92) and RH (r = 0.92), but oppositely with temperature (r = −0.92). Nanjing wintertime nitrate behaved similarly as it did during summer, with correlation coefficients of r = 0.89 with K_p, r = 0.93 with RH, and r = −0.90 with temperature. As is well known, low temperature and high RH favor the thermodynamic gas/particle partitioning of NH_4NO_3, thus these results verify that homogenous reaction between ammonia and nitric acid was the dominant mechanism controlling nitrate formation during both summer and winter in Nanjing. Note that the nitrate variations did not respond to the changes of solar radiation, indicating that photochemical activities did not directly influence the nitrate formation in Nanjing. We propose this nitrate formation mechanism as "*Type I—thermodynamics driven*".

In the case of Beijing, nitrate in summer generally also matched well with the thermodynamic parameters (r = 0.84 with K_p, r = 0.88 with RH, and r = −0.89 with temperature). On the contrary, wintertime nitrate correlated oppositely with these parameters (r = −0.67 with K_p, r = −0.34 with RH, and r = 0.58 with temperature), but positively responded to the increase of solar radiation during daytime, reflecting the dominant contribution from photochemical production over thermodynamic gas/particle partitioning. This mechanism is also proposed by Sun et al. [29], and here we define it as "*Type II—photochemistry driven*".

In the case of Lanzhou, the nitrate diurnal pattern during summer had no correlations with K_p (r = −0.02), temperature (r = −0.09), and RH (r = 0.15), indicating an insignificant role of gas/particle partitioning (Type I); although no solar radiation data was available, the sharp decrease of nitrate during afternoon demonstrated that it was not associated with photochemical production too (Type II). Xu et al. [31] interpreted that the dynamics of planetary boundary layer (PBL) and down-mixing of nitrate produced from nocturnal chemistry in the morning, likely caused such nitrate behavior during summer in Lanzhou. This behavior is also likely related with the specific topography of Lanzhou, as a prior study reported that pollution of secondary species could be enhanced due to mountain trapping [42]. This mechanism is defined as "*Type III—PBL dynamics driven*". Nitrate in Lanzhou during winter had negative correlations with the thermodynamic parameters (r = −0.80 with K_p,

$r = -0.93$ with RH, and $r = 0.91$ with temperature); it also had an afternoon peak, indicating it was mainly driven by photochemical production (Type II)—a mechanism proposed by Xu et al. [32] as well.

Here we propose three types of mechanisms that can govern urban aerosol nitrate formation. However, it should be noted that there are likely other mechanisms. For example, Yang et al. [43] showed that transportation of haze from other regions could lead to the high nitrate concentrations observed in Beijing.

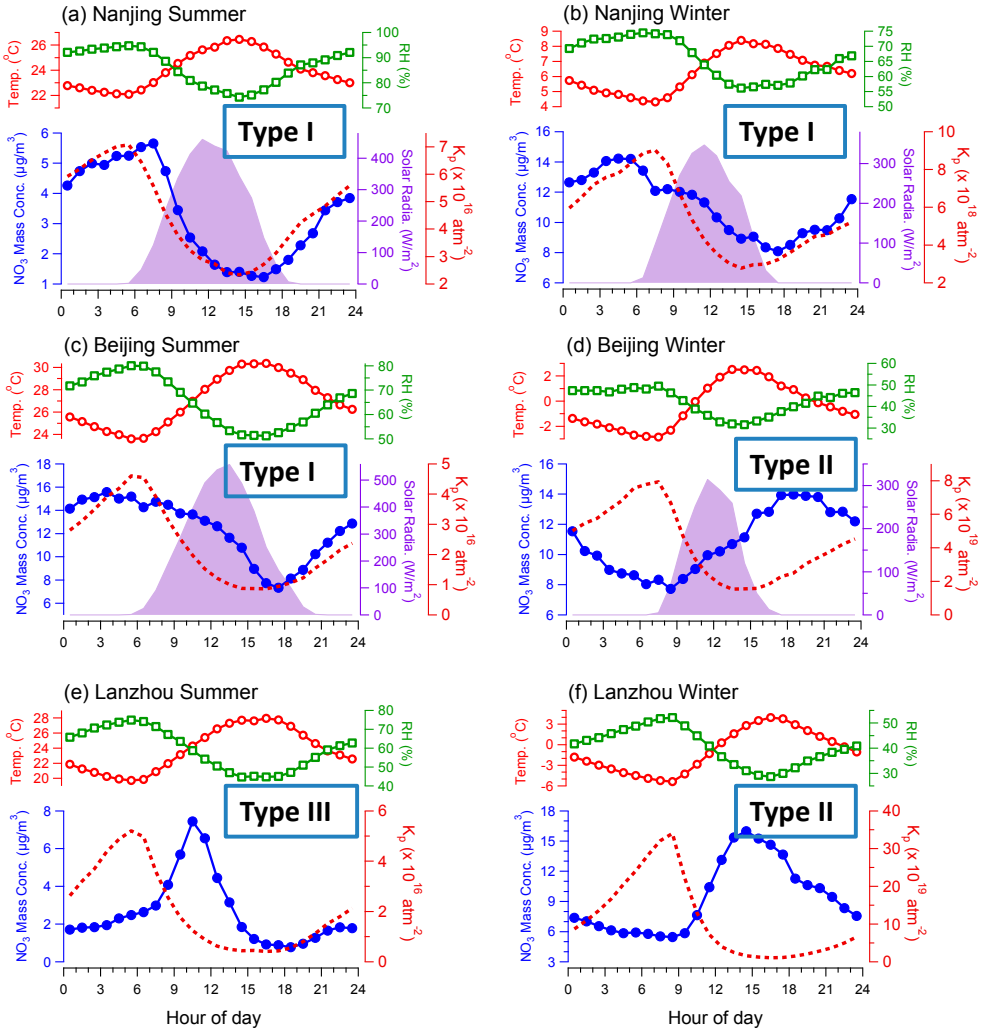

Figure 3. Diurnal patterns of temperature (top panel, left *y* axis), relative humidity (RH) (top panel, right *y* axis), nitrate concentration (bottom panel, left *y* axis), solar radiation and equilibrium constant (K_p) of ammonium nitrate (bottom panel, right *y* axis) ($K_p = K_p(298)\exp\left\{a\left(\frac{298}{T}-1\right)+b\left[1+\ln\left(\frac{298}{T}\right)-\frac{298}{T}\right]\right\}$, for reaction $NH_4NO_3(p) \leftrightarrow NH_3(g) + HNO_3(g)$. $K_p(298)$ is the equilibrium constant at 298 K (3.36×10^{16} atm^{-2}), a = 75.11 and b = −13.5 [16]): (**a**) Nanjing summer, (**b**) Nanjing winter, (**c**) Beijing summer, (**d**) Beijing winter, (**e**) Lanzhou summer, and (**f**) Lanzhou winter. (Type I—thermodynamics driven; Type II—photochemistry driven; Type III—PBL dynamics driven. Please refer to the main text for more details).

3.2. *Influences of Other Aerosol Components*

Due to influences of other aerosol components including primary species directly emitted from various sources, and the secondary components produced by different pathways, the mass contributions of nitrate to PM_1 may vary greatly at different pollution levels. In Figure 4, we plotted the mass percentages of nitrate against the total PM_1 concentrations (divided into a number of bins).

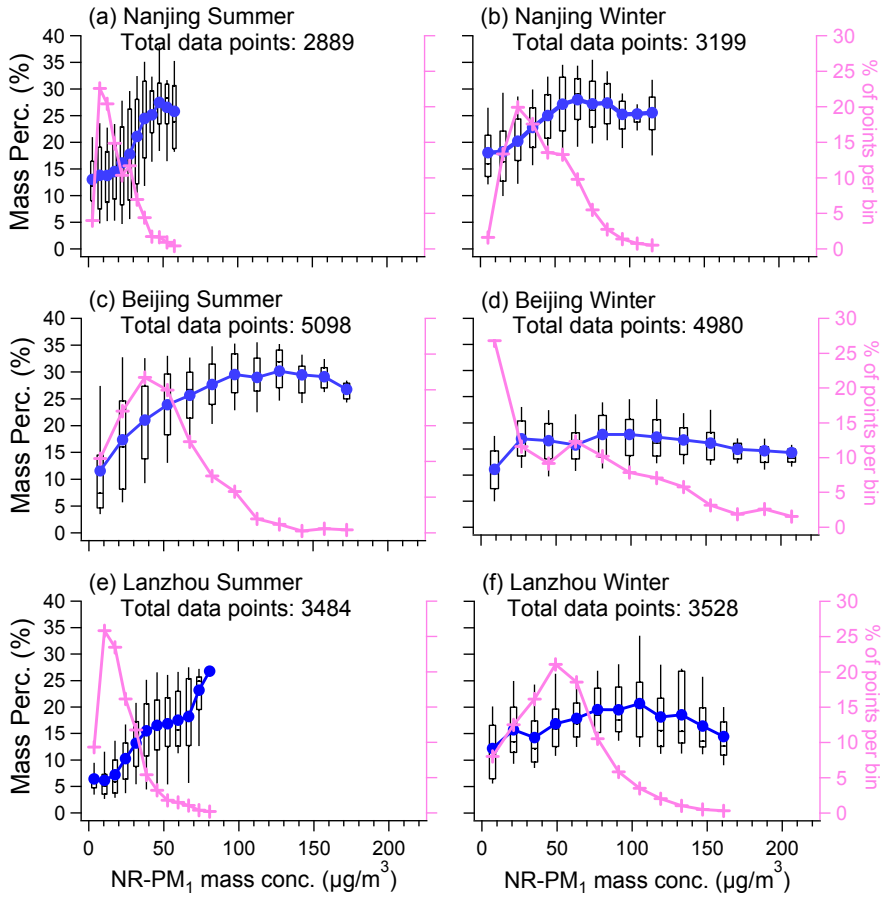

Figure 4. Variations of the mass percentages of nitrate as a function of the total non-refractory PM_1 ($NR\text{-}PM_1$)concentrations (left *y* axis, note the $NR\text{-}PM_1$ did not include *r*BC for all datasets in this figure), and the percentage of data points in each bin (right *y* axis): (**a**) Nanjing summer, (**b**) Nanjing winter, (**c**) Beijing summer, (**d**) Beijing winter, (**e**) Lanzhou summer, and (**f**) Lanzhou winter (the box plot symbols are the same as those described in Figure 1; note Figure 4c–f are reproduced and modified from previous studies [28,29,31,32]).

For Nanjing summer, besides a small pool of data (1.3% of total) with PM_1 concentrations exceeding 50 $\mu g/m^3$, the mass fractions of nitrate increased with the increase of PM_1 mass loadings. Generally, this finding is consistent with the measurement results of Zhang et al. [37] during summer in Nanjing. The data of Lanzhou during summer showed a more obvious increasing trend, as shown in Figure 4e. For Beijing, for the majority of data (98.7% of total), nitrate concentrations also displayed an increasing trend. Nitrate concentrations decreased slightly (from 30% to 27%) only for some extremely polluted periods (1.3% of total). These results suggest that although nitrate concentrations were overall low, as it is easy to evaporate due to high temperatures in summer, the contribution of nitrate to PM_1 is generally higher during polluted periods than during periods of clean(er) air. This finding highlights the importance of NO_x emission control (such as from traffic or industry) to reduce nitrate concentrations during heavy haze events in summer.

On the other hand, wintertime nitrate behaviors were different. First, on average, the fluctuations were smaller during winter than during summer—Nanjing: summer (13%–28%) versus winter (18%–28%), Beijing: summer (11%–30%) versus winter (11%–18%), Lanzhou: summer (6%–27%) versus winter (12%–21%). Secondly, the relative contributions of nitrate presented a general trend which increased first then decreased with the increase of PM_1 concentrations. Different from summer where the nitrate mass fractions decreased only for a very small fraction of data, the decrease in nitrate fractions during winter occurred for a much larger portion of data (~11% in Nanjing, ~22% in

Beijing, and ~4% in Lanzhou). This wintertime "increase-decrease" nitrate behavior was confirmed by other studies, such as a study by Yao et al. during winter in Lanzhou [41]. For Nanjing in winter, further analyses demonstrated that the elevation of primary organic aerosol (OA) contributions was an important reason causing the decrease in nitrate fractions at high PM_1 loadings. Sun et al. [29] found that for winter in Beijing, the decrease in nitrate fractions were mainly due to increases in contributions from sulfate and OAs (especially primary OAs, such as coal combustion OAs), and the aqueous-phase oxidation pathway likely contributed significantly to sulfate [30]. In the case of winter in Lanzhou, Xu et al. [32] showed that the increased contribution from primary OAs (including biomass burning OAs, coal combustion OAs, traffic- and cooking-related OAs) led to the decrease in nitrate fractions at high PM_1 concentrations. These results point out the need and importance of emission control of the primary sources in urban areas during hazy days. The results also suggest that emission control of secondary aerosol gaseous precursors in some areas is likely also important, as the production of secondary species (including both inorganic and organic species [44–46]) might be enhanced during hazy days. This is also proposed by Huang et al. [9] based on the $PM_{2.5}$ results for a few Chinese megacities during January 2013.

3.3. Competition with Ammonium Sulfate/Bisulfate

For submicron aerosols, nitrate is overwhelmingly present in the form of NH_4NO_3 rather than other metal nitrates. NH_4NO_3 is formed from the neutralization of HNO_3 with NH_3. However, under real atmospheric conditions, HNO_3 has to compete with H_2SO_4, as NH_3 tends to first react with H_2SO_4 thermodynamically. Previous studies show that NH_4NO_3 can start to form when the molar ratio of ${NH_4}^+/{SO_4}^{2-}$ is larger than 1.5 (ammonium-rich). In fact, we found that the molar ratios of ${NH_4}^+/{SO_4}^2$ for the AMS data investigated here were in most cases larger than 2. Note that due to possible influences from reaction of NH_3 with HCl (although it was likely minor, as chloride fractions were much lower than those of nitrate and sulfate), the ${NH_4}^+$ molar concentrations calculated here excluded the portions that were neutralized by HCl. The results indicate the abundance of ammonia, which is favorable for nitrate formation. This is different from the filter-based $PM_{2.5}$ results reported by Ye et al. [20] in Shanghai, from where a large portion of data was in the ammonium-poor regions (${NH_4}^+/{SO_4}^{2-} < 1.5$), especially during summer and autumn.

In order to further investigate the relationship between NH_4NO_3, NH_4HSO_4, and $(NH_4)_2SO_4$, we define an excess molar ${NH_4}^+$ relative to $(NH_4)_2SO_4$: Excess ${NH_4}^+ = ({NH_4}^+/{SO_4}^{2-} - 2) \times {SO_4}^{2-}$. In Figure 5, we show the scatter plots of the excess molar ${NH_4}^+$ concentrations versus molar concentrations of nitrate for all datasets. In this figure, a slope larger than 1 means that NH_4NO_3 forms when sulfuric acid is fully neutralized by ammonia (namely, ammonium sulfate). A slope with a positive value but less than 1 means that partial ${NH_4}^+$ is associated with bisulfate in addition to nitrate. As $(NH_4)_2SO_4$ plus any fraction of NH_4HSO_4 can result in a compound with the ${NH_4}^+/{SO_4}^2$ stoichiometric ratio larger than 1.5—that of $(NH_4)_3H(SO_4)_2$, in this case, it therefore means that NH_4NO_3 can start to form after the formation of $(NH_4)_3H(SO_4)_2$. The correlations shown in Figure 5 are generally strong (r^2 of 0.84–0.96), but it should be noted that the fitted slopes only represent the statistical average values. For each individual dataset, there are data points with molar ratios larger or less than 1 (especially for Beijing winter), and the deviations of fitted lines from 1:1 lines are sometimes subtle; for instance the slopes of Beijing Winter (1.02) and Lanzhou summer (0.98) datasets are very close to 1. Nevertheless, from a statistical standpoint, on average, during summer in Nanjing, and during both summer and winter in Beijing, nitrate seemed significantly likely to be generated following the formation of $(NH_4)_2SO_4$, while it was able to form after the formation of $(NH_4)_3H(SO_4)_2$ during winter in Nanjing, and during both summer and winter in Lanzhou.

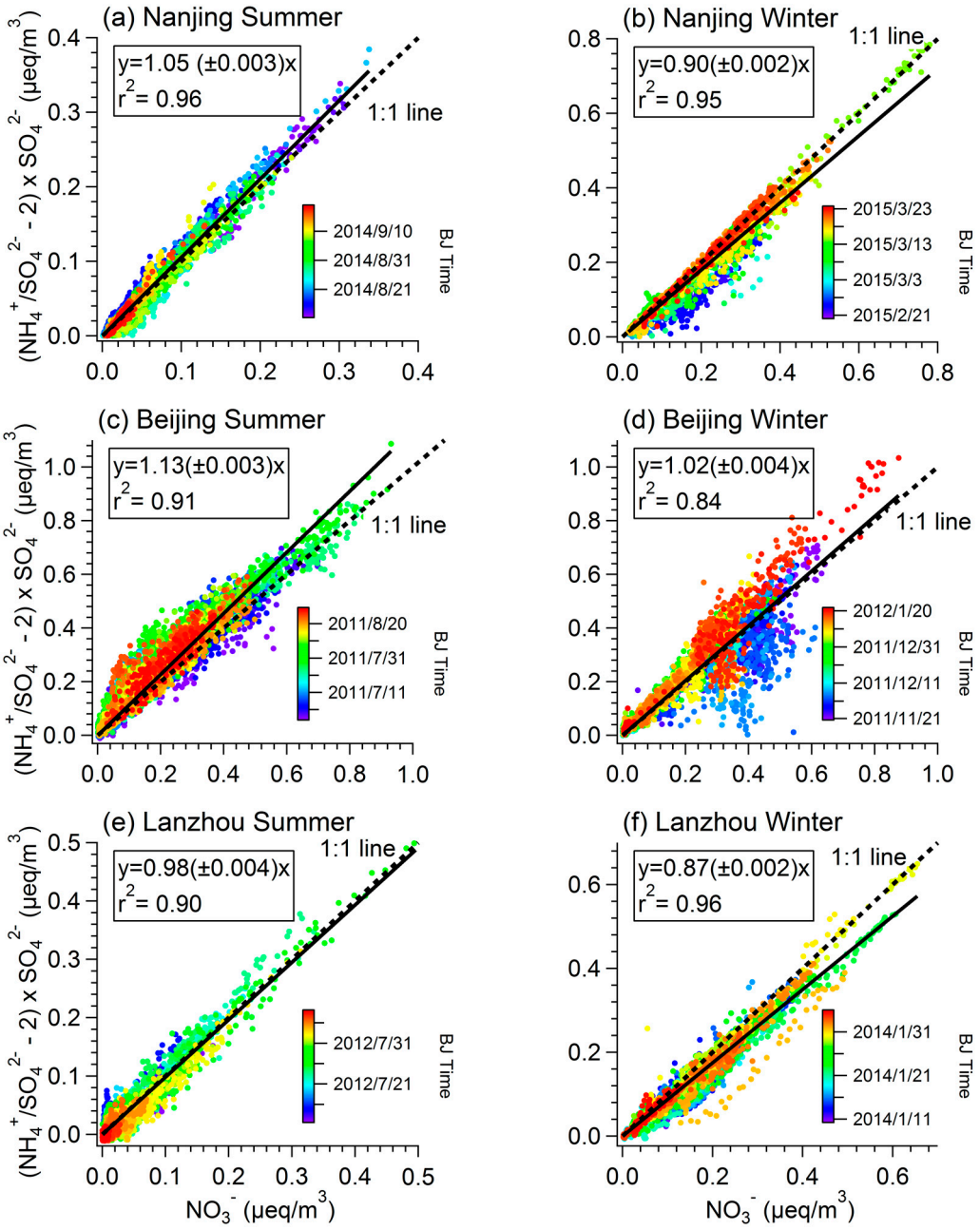

Figure 5. Scatter plots of the molar concentrations of excess NH_4^+ relative to $(NH_4)_2SO_4$ versus NO_3^- (the NH_4^+ molar concentrations were the measured NH_4^+ molar concentrations minus the amounts used to neutralize HCl): (**a**) Nanjing summer, (**b**) Nanjing winter, (**c**) Beijing summer, (**d**) Beijing winter, (**e**) Lanzhou summer, and (**f**) Lanzhou winter (data pointes were colored by time).

4. Conclusions

This work investigated the characteristics and formation mechanisms of fine aerosol nitrate in typical urban areas of China using the Aerodyne AMS data collected in Nanjing, Beijing, and Lanzhou, during both summer and winter. Results showed that nitrate could occupy up to a quarter of urban PM_1 mass, with concentrations that were typically higher than those found in rural/remote regions. During summer, the relative mass contributions of nitrate generally increased with the increase of PM_1 mass loadings, highlighting the importance of NO_x emission control; during winter, nitrate contributions increased first then decreased with the increase of PM_1 concentrations, with the decrease likely caused by the increases of both primary and secondary species, suggesting that control of both

primary particles and secondary aerosol precursors is essential for effectively reducing the heavy haze pollution. Furthermore, by investigating the relationships between the diurnal patterns of nitrate and those of meteorological parameters, etc., we proposed three types of mechanisms that can govern the nitrate variations in urban China: "Type I—thermodynamics driven", "Type II—photochemistry driven", and "Type III—PBL dynamics driven". Competition between the formation of ammonium nitrate and ammonium bisulfate/sulfate were discussed, and we found that NH_4NO_3 could start to form before sulfuric acid was fully neutralized and after $(NH_4)_3H(SO_4)_2$ was formed.

Overall, this work provides useful insights into nitrate formation, and thus is valuable for reducing aerosol nitrate pollution. The three types of mechanisms we proposed are valuable to aid in the interpretation of nitrate behaviors documented in other studies. Nevertheless, this study indicates that nitrate formation can be complex, and does not exclude other mechanisms. Different nitrate pollution events occurring in the same location might be dominated by different mechanisms as well [43]. Future work is thus still necessary to carefully elucidate the atmospheric behaviors of nitrate under different atmospheric environments.

Acknowledgments: This work was financially supported by the Natural Science Foundation of China (21407079, 21577065, and 91544220), Jiangsu Natural Science Foundation (BK20150042), Jiangsu Provincial Specially-Appointed Professors Foundation, Jiangsu Innovation and Entrepreneurship Program, and the Startup Foundation for Introducing Talent of NUIST (2014r064).

Author Contributions: Xinlei Ge conceived the idea; Xinlei Ge and Yanan He wrote the manuscript; Xinlei Ge, Yanan He, and Junfeng Wang performed Nanjing field measurements and data analyses; Yele Sun provided Beijing data, and Jianzhong Xu provided Lanzhou data; Yafei Shen and Mindong Chen provided valuable comments and suggestions for the development of the manuscript.

Conflicts of Interest: The authors declare no conflict of interest.

References

1. Hu, J.; Ying, Q.; Wang, Y.; Zhang, H. Characterizing multi-pollutant air pollution in China: Comparison of three air quality indices. *Environ. Int.* **2015**, *84*, 17–25. [CrossRef] [PubMed]
2. Qi, L.; Chen, M.; Ge, X.; Zhang, Y.; Guo, B. Seasonal variations and sources of 17 aerosol metal elements in suburban Nanjing, China. *Atmosphere* **2016**, *7*, 153. [CrossRef]
3. Zhang, Y.; Cao, F. Fine particulate matter (PM2.5) in China at a city level. *Sci. Rep.* **2015**, *5*, 14884. [CrossRef] [PubMed]
4. Griffith, S.M.; Huang, X.H.H.; Louie, P.K.K.; Yu, J. Characterizing the thermodynamic and chemical composition factors controlling PM2.5 nitrate: Insights gained from two years of online measurements in Hong Kong. *Atmos. Environ.* **2015**, *122*, 864–875. [CrossRef]
5. Putaud, J.P.; Van Dingenen, R.; Alastuey, A.; Bauer, H.; Birmili, W.; Cyrys, J.; Flentje, H.; Fuzzi, S.; Gehrig, R.; Hansson, H.C.; et al. A European aerosol phenomenology—3: Physical and chemical characteristics of particulate matter from 60 rural, urban, and kerbside sites across Europe. *Atmos. Environ.* **2010**, *44*, 1308–1320. [CrossRef]
6. Pan, Y.; Wang, Y.; Zhang, J.; Liu, Z.; Wang, L.; Tian, S.; Tang, G.; Gao, W.; Ji, D.; Song, T.; et al. Redefining the importance of nitrate during haze pollution to help optimize an emission control strategy. *Atmos. Environ.* **2016**, *141*, 197–202. [CrossRef]
7. Liang, C.; Duan, F.; He, K.; Ma, Y. Review on recent progress in observations, source identifications and countermeasures of PM2.5. *Environ. Int.* **2016**, *86*, 150–170. [CrossRef] [PubMed]
8. Yin, J.; Harrison, R.M. Pragmatic mass closure study for PM1.0, PM2.5 and PM10 at roadside, urban background and rural sites. *Atmos. Environ.* **2008**, *42*, 980–988. [CrossRef]
9. Huang, R.; Zhang, Y.; Bozzetti, C.; Ho, K.; Cao, J.; Han, Y.; Daellenbach, K.R.; Slowik, J.G.; Platt, S.M.; Canonaco, F.; et al. High secondary aerosol contribution to particulate pollution during haze events in China. *Nature* **2014**, *514*, 218–222. [CrossRef] [PubMed]
10. Ottley, C.J.; Harrison, R.M. The spatial distribution and particle size of some inorganic nitrogen, sulphur and chlorine species over the North Sea. *Atmos. Environ.* **1992**, *26*, 1689–1699. [CrossRef]
11. Mather, T.A.; Allen, A.G.; Davison, B.M.; Pyle, D.M.; Oppenheimer, C.; McGonigle, A.J.S. Nitric acid from volcanoes. *Earth Planet. Sci. Lett.* **2004**, *218*, 17–30. [CrossRef]

12. Hertel, O.; Skjoth, C.A.; Reis, S.; Bleeker, A.; Harrison, R.M.; Cape, J.N.; Fowler, D.; Skiba, U.; Simpson, D.; Jickells, T.; et al. Governing processes for reactive nitrogen compounds in the European atmosphere. *Biogeosciences* **2012**, *9*, 4921–4954. [CrossRef]
13. Mentel, T.F.; Bleilebens, D.; Wahner, A. A study of nighttime nitrogen oxide oxidation in a large reaction chamber—The fate of NO_2, N_2O_5, HNO_3, and O_3 at different humidities. *Atmos. Environ.* **1996**, *30*, 4007–4020. [CrossRef]
14. Dall'Osto, M.; Harrison, R.M.; Coe, H.; Williams, P. Real-time secondary aerosol formation during a fog event in London. *Atmos. Chem. Phys.* **2009**, *9*, 2459–2469. [CrossRef]
15. Petetin, H.; Sciare, J.; Bressi, M.; Gros, V.; Rosso, A.; Sanchez, O.; Sarda-Estève, R.; Petit, J.E.; Beekmann, M. Assessing the ammonium nitrate formation regime in the Paris megacity and its representation in the CHIMERE model. *Atmos. Chem. Phys.* **2016**, *16*, 10419–10440. [CrossRef]
16. Seinfeld, J.H.; Pandis, S.N. *Atmospheric Chemistry and Physics: From Air Pollution to Climate Change*; John Wiley & Sons: New York, NY, USA, 2006.
17. Huang, X.; Qiu, R.; Chan, C.K.; Ravi Kant, P. Evidence of high PM2.5 strong acidity in ammonia-rich atmosphere of Guangzhou, China: Transition in pathways of ambient ammonia to form aerosol ammonium at $[NH_4^+]/[SO_4^{2-}] = 1.5$. *Atmos. Res.* **2011**, *99*, 488–495. [CrossRef]
18. Pathak, R.K.; Wu, W.S.; Wang, T. Summertime $PM_{2.5}$ ionic species in four major cities of China: Nitrate formation in an ammonia-deficient atmosphere. *Atmos. Chem. Phys.* **2009**, *9*, 1711–1722. [CrossRef]
19. He, K.; Zhao, Q.; Ma, Y.; Duan, F.; Yang, F.; Shi, Z.; Chen, G. Spatial and seasonal variability of PM2.5 acidity at two Chinese megacities: Insights into the formation of secondary inorganic aerosols. *Atmos. Chem. Phys.* **2012**, *12*, 1377–1395. [CrossRef]
20. Tao, Y.; Ye, X.; Ma, Z.; Xie, Y.; Wang, R.; Chen, J.; Yang, X.; Jiang, S. Insights into different nitrate formation mechanisms from seasonal variations of secondary inorganic aerosols in Shanghai. *Atmos. Environ.* **2016**, *145*, 1–9. [CrossRef]
21. Canagaratna, M.R.; Jayne, J.T.; Jimenez, J.L.; Allan, J.D.; Alfarra, M.R.; Zhang, Q.; Onasch, T.B.; Drewnick, F.; Coe, H.; Middlebrook, A.; et al. Chemical and microphysical characterization of ambient aerosols with the aerodyne aerosol mass spectrometer. *Mass Spectrom. Rev.* **2007**, *26*, 185–222. [CrossRef] [PubMed]
22. Jimenez, J.L.; Canagaratna, M.R.; Donahue, N.M.; Prevot, A.S.H.; Zhang, Q.; Kroll, J.H.; DeCarlo, P.F.; Allan, J.D.; Coe, H.; Ng, N.L.; et al. Evolution of organic aerosols in the atmosphere. *Science* **2009**, *326*, 1525–1529. [CrossRef] [PubMed]
23. Onasch, T.B.; Trimborn, A.; Fortner, E.C.; Jayne, J.T.; Kok, G.L.; Williams, L.R.; Davidovits, P.; Worsnop, D.R. Soot particle aerosol mass spectrometer: Development, validation, and initial application. *Aerosol Sci. Technol.* **2012**, *46*, 804–817. [CrossRef]
24. Wang, J.; Ge, X.; Chen, Y.; Shen, Y.; Zhang, Q.; Sun, Y.; Xu, J.; Ge, S.; Yu, H.; Chen, M. Highly time-resolved urban aerosol characteristics during springtime in Yangtze River Delta, China: Insights from soot particle aerosol mass spectrometry. *Atmos. Chem. Phys.* **2016**, *16*, 9109–9127. [CrossRef]
25. Wang, J.; Onasch, T.B.; Ge, X.; Collier, S.; Zhang, Q.; Sun, Y.; Yu, H.; Chen, M.; Prévôt, A.S.H.; Worsnop, D.R. Observation of Fullerene Soot in Eastern China. *Environ. Sci. Technol. Lett.* **2016**, *3*, 121–126. [CrossRef]
26. Ng, N.L.; Herndon, S.C.; Trimborn, A.; Canagaratna, M.R.; Croteau, P.L.; Onasch, T.B.; Sueper, D.; Worsnop, D.R.; Zhang, Q.; Sun, Y.L.; et al. An Aerosol Chemical Speciation Monitor (ACSM) for Routine Monitoring of the Composition and Mass Concentrations of Ambient Aerosol. *Aerosol Sci. Technol.* **2011**, *45*, 770–784. [CrossRef]
27. DeCarlo, P.F.; Kimmel, J.R.; Trimborn, A.; Northway, M.J.; Jayne, J.T.; Aiken, A.C.; Gonin, M.; Fuhrer, K.; Horvath, T.; Docherty, K.S.; et al. Field-deployable, high-resolution, time-of-flight aerosol mass spectrometer. *Anal. Chem.* **2006**, *78*, 8281–8289. [CrossRef] [PubMed]
28. Sun, Y.; Wang, Z.; Dong, H.; Yang, T.; Li, J.; Pan, X.; Chen, P.; Jayne, J.T. Characterization of summer organic and inorganic aerosols in Beijing, China with an Aerosol Chemical Speciation Monitor. *Atmos. Environ.* **2012**, *51*, 250–259. [CrossRef]
29. Sun, Y.L.; Wang, Z.F.; Fu, P.Q.; Yang, T.; Jiang, Q.; Dong, H.B.; Li, J.; Jia, J.J. Aerosol composition, sources and processes during wintertime in Beijing, China. *Atmos. Chem. Phys.* **2013**, *13*, 4577–4592. [CrossRef]
30. Sun, Y.; Wang, Z.; Fu, P.; Jiang, Q.; Yang, T.; Li, J.; Ge, X. The impact of relative humidity on aerosol composition and evolution processes during wintertime in Beijing, China. *Atmos. Environ.* **2013**, *77*, 927–934. [CrossRef]

31. Xu, J.; Zhang, Q.; Chen, M.; Ge, X.; Ren, J.; Qin, D. Chemical composition, sources, and processes of urban aerosols during summertime in northwest China: Insights from high-resolution aerosol mass spectrometry. *Atmos. Chem. Phys.* **2014**, *14*, 12593–12611. [CrossRef]
32. Xu, J.; Shi, J.; Zhang, Q.; Ge, X.; Canonaco, F.; Prévôt, A.S.H.; Vonwiller, M.; Szidat, S.; Ge, J.; Ma, J.; et al. Wintertime organic and inorganic aerosols in Lanzhou, China: Sources, processes, and comparison with the results during summer. *Atmos. Chem. Phys.* **2016**, *16*, 14937–14957. [CrossRef]
33. Farmer, D.K.; Matsunaga, A.; Docherty, K.S.; Surratt, J.D.; Seinfeld, J.H.; Ziemann, P.J.; Jimenez, J.L. Response of an aerosol mass spectrometer to organonitrates and organosulfates and implications for atmospheric chemistry. *Proc. Natl. Acad. Sci. USA* **2010**, *107*, 6670–6675. [CrossRef] [PubMed]
34. Paatero, P.; Tapper, U. Positive matrix factorization: A non-negative factor model with optimal utilization of error estimates of data values. *Environmetrics* **1994**, *5*, 111–126. [CrossRef]
35. Zhang, Q.; Jimenez, J.; Canagaratna, M.; Ulbrich, I.; Ng, N.; Worsnop, D.; Sun, Y. Understanding atmospheric organic aerosols via factor analysis of aerosol mass spectrometry: A review. *Anal. Bioanal. Chem.* **2011**, *401*, 3045–3067. [CrossRef] [PubMed]
36. Li, Y.J.; Lee, B.P.; Su, L.; Fung, J.C.H.; Chan, C.K. Seasonal characteristics of fine particulate matter (PM) based on high-resolution time-of-flight aerosol mass spectrometric (HR-ToF-AMS) measurements at the HKUST Supersite in Hong Kong. *Atmos. Chem. Phys.* **2015**, *15*, 37–53. [CrossRef]
37. Zhang, Y.J.; Tang, L.L.; Wang, Z.; Yu, H.X.; Sun, Y.L.; Liu, D.; Qin, W.; Canonaco, F.; Prévôt, A.S.H.; Zhang, H.L.; et al. Insights into characteristics, sources, and evolution of submicron aerosols during harvest seasons in the Yangtze River delta region, China. *Atmos. Chem. Phys.* **2015**, *15*, 1331–1349. [CrossRef]
38. Zhang, Y.J.; Tang, L.; Yu, H.; Wang, Z.; Sun, Y.; Qin, W.; Chen, W.; Chen, C.; Ding, A.; Wu, J.; et al. Chemical composition, sources and evolution processes of aerosol at an urban site in Yangtze River Delta, China during wintertime. *Atmos. Environ.* **2016**, *123*, 339–349. [CrossRef]
39. Sun, Y.; Du, W.; Fu, P.; Wang, Q.; Li, J.; Ge, X.; Zhang, Q.; Zhu, C.; Ren, L.; Xu, W.; et al. Primary and secondary aerosols in Beijing in winter: Sources, variations and processes. *Atmos. Chem. Phys.* **2016**, *16*, 8309–8329. [CrossRef]
40. Sun, Y.L.; Wang, Z.F.; Du, W.; Zhang, Q.; Wang, Q.Q.; Fu, P.Q.; Pan, X.L.; Li, J.; Jayne, J.; Worsnop, D.R. Long-term real-time measurements of aerosol particle composition in Beijing, China: Seasonal variations, meteorological effects, and source analysis. *Atmos. Chem. Phys.* **2015**, *15*, 10149–10165. [CrossRef]
41. Zhang, X.; Zhang, Y.; Sun, J.; Yu, Y.; Canonaco, F.; Prévôt, A.S.H.; Li, G. Chemical characterization of submicron aerosol particles during wintertime in a northwest city of China using an Aerodyne aerosol mass spectrometry. *Environ. Pollut.* **2017**. [CrossRef] [PubMed]
42. Yao, T.; Fung, J.C.H.; Ma, H.; Lau, A.K.H.; Chan, P.W.; Yu, J.Z.; Xue, J. Enhancement in secondary particulate matter production due to mountain trapping. *Atmos. Res.* **2014**, 147–148, 227–236. [CrossRef]
43. Yang, T.; Sun, Y.; Zhang, W.; Wang, Z.; Liu, X.; Fu, P.; Wang, X. Evolutionary processes and sources of high-nitrate haze episodes over Beijing, Spring. *J. Environ. Sci.* **2016**. [CrossRef]
44. Ge, X.; Zhang, Q.; Sun, Y.; Ruehl, C.R.; Setyan, A. Effect of aqueous-phase processing on aerosol chemistry and size distributions in Fresno, California, during wintertime. *Environ. Chem.* **2012**, *9*, 221–235. [CrossRef]
45. Gilardoni, S.; Massoli, P.; Paglione, M.; Giulianelli, L.; Carbone, C.; Rinaldi, M.; Decesari, S.; Sandrini, S.; Costabile, F.; Gobbi, G.P.; et al. Direct observation of aqueous secondary organic aerosol from biomass-burning emissions. *Proc. Natl. Aacd. Sci. USA* **2016**, *113*, 10013–10018. [CrossRef] [PubMed]
46. Ervens, B.; Turpin, B.J.; Weber, R.J. Secondary organic aerosol formation in cloud droplets and aqueous particles (aqSOA): A review of laboratory, field and model studies. *Atmos. Chem. Phys.* **2011**, *11*, 11069–11102. [CrossRef]